Chemical Science

ROYAL SOCIETY OF CHEMISTRY

EDGE ARTICLE

View Article Online
View Journal | View Issue

Cite this: *Chem. Sci.*, 2022, **13**, 13623

All publication charges for this article have been paid for by the Royal Society of Chemistry

Unexpected chirality transition and inversion mediated by dissolution–aggregation and the odd–even effect†

Yafei Ma, Xiaoxiao Cheng,* Haotian Ma, Zixiang He, Zhengbiao Zhang and Wei Zhang *

Received 21st September 2022
Accepted 25th October 2022

DOI: 10.1039/d2sc05255e

rsc.li/chemical-science

The evolution of hierarchical chirality at macromolecular and supramolecular levels in biological systems is ubiquitous; however, achieving precise control over transitions between them in polymer systems is still challenging. Here, we reported multiple chiroptical transitions and inversion phenomena in side-chain azobenzene (Azo) polymers, PAzo-L/D-*m* (*m* = 3, 6, 7, 8, 9, and 10, where *m* is the total number of atoms from the chiral stereocenter to the Azo unit), with different distances from the chiral stereocenter to the Azo unit. In the case of *m* = 3, an unexpected macromolecular-to-supramolecular chirality transition and inversion occurred *in situ* when the Azo-polymer underwent from a macromolecular-dissolved state to a supramolecular-aggregated state. To our surprise, an exciton-coupling induced multiple chiroptical inversion was observed upon the heating-assisted reassembly treatment, which was demonstrated to be driven by *H*- to *J*-aggregation transition. Furthermore, the odd–even effect was first established to regulate the supramolecular helical orientations (left- or right-handedness) in side-chain Azo-polymer assemblies.

Introduction

Chirality is one of the most-studied topics due to its ubiquitous presence in biological systems, such as proteins, DNA, enzymes, *etc.*[1–4] Chirality can be expressed in polymer systems at different levels, including primary chirality (configurational chirality), secondary chirality (conformational chirality/helical macromolecular conformation), tertiary chirality (supramolecular chirality in aggregates), and fourth-level chirality (object chirality).[5–7] Considering that the expression of high-level chirality is usually determined by lower chiral elements, the controlled regulation of multi-level chirality is very important. In polymer systems, the efforts on chirality control mainly focus on secondary macromolecular chirality and tertiary supramolecular chirality in aggregated states. In the past few years, the studies on chirality control have been mainly involved in the topics of chirality amplification, chirality switching and chirality inversion, among which the reversible chirality inversion of left-handedness (M) and right-handedness (P) is considered to be the most fascinating and unique phenomenon.[8,9] The inversion of primary chirality requires the breaking and formation of covalent bonds, while the inversion of secondary and tertiary chirality can be achieved only by a delicate balance of various non-covalent interactions. Precise regulation of chirality inversion through both various external stimuli (*e.g.*, light,[10–12] temperature[13,14] and solvent[15–18]) and internal structure changes (*e.g.*, absolute configuration,[19–21] chemical modification[22] and the odd–even effect[23–28]) may lead to further understanding of chirality transition in biological systems and expanding its potential applications.

Although the transition between the secondary chirality and tertiary chirality in polymers plays an important role in nature, the interactive connection of the above two different hierarchical chiralities has been rarely studied. The control of chirality inversion in polymer systems mainly focuses on the regulation of the helical conformation of the main-chain conjugated polymers in a dissolved state[29–33] or supramolecular chirality of polymer assemblies in an aggregated state.[34,35] Malashkevich *et al.* reported that macromolecular-to-supramolecular helicity inversion existed in cartilage oligomeric matrix proteins. These peptide chains were mainly folded into right-handed α helices and wrapped around each other in a left-handed superhelix.[36] This discovery provided a new perspective for achieving controlled chirality transition from a macromolecular to a supramolecular level in polymer aggregates.

In this work, the target is to step forward and bridge the relationship gap between the dynamic inversion behavior of macromolecular chirality governed by covalent bonds and supramolecular chirality stabilized by non-covalent bonds, which should be applied to side-chain helical polymers and not only to

State and Local Joint Engineering Laboratory for Novel Functional Polymeric Materials, Jiangsu Engineering Laboratory of Novel Functional Polymeric Materials, Suzhou Key Laboratory of Macromolecular Design and Precision Synthesis, College of Chemistry, Chemical Engineering and Materials Science, Soochow University, Suzhou, 215123, Jiangsu, China. E-mail: weizhang@suda.edu.cn; xxcheng@suda.edu.cn

† Electronic supplementary information (ESI) available. See DOI: https://doi.org/10.1039/d2sc05255e

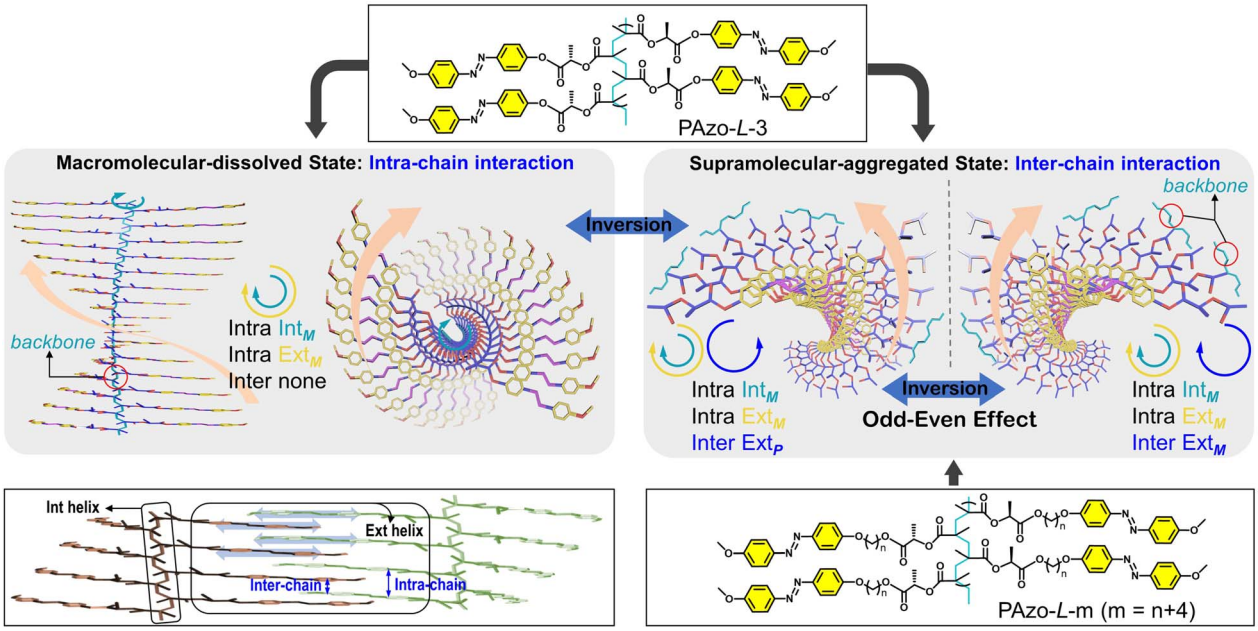

Scheme 1 Schematic presentation of chirality control for side-chain engineering (L-configuration, m = 6, 7, 8, 9, and 10) by dissolution–aggregation differentiations and the odd–even effect. The internal helical backbone is denoted as Int_M and the external helix defined by the Azo units is denoted as Ext_M and Ext_P. The abbreviations "intra" and "intra" are the intra-chain and inter-chain, respectively.

the main-chain helical ones. To fulfill this demand, we investigated the chirality transition behaviours in side-chain Azo-polymers (Scheme 1, PAzo-L/D-m, m = 3, 6, 7, 8, 9, and 10) with different distances from the chiral stereocenter to the Azo unit. The results indicated that there were three types of chiral properties that existed in the system, for example, an intra-chain internal helical backbone and intra-chain and inter-chain external helical Azo units. The unexpected macromolecular-to-supramolecular chirality inversion was found when PAzo-L/D-3 went from a completely dissolved-state to an aggregated-state. Interestingly, multiple chirality inversions were successfully realized with the help of heating-assisted reassembly treatment, which can be used to build chiroptical switches with multiple inversion properties. Meanwhile, the odd–even effect was first established to control the supramolecular helical orientations of Azo units in this series of chiral Azo-polymer aggregates.

Results and discussion

In order to study the interactive connection of helical macromolecular conformation and supramolecular chirality, a series of Azo-polymers were synthesized by reversible addition–fragmentation chain transfer (RAFT) polymerization (Scheme S1†). The results of NMR, chiral high-performance liquid chromatography (HPLC) and other characterization studies agreed well with the Azo monomer and polymer structures (Fig. S1–S3†). The circular dichroism (CD) and UV-vis spectra of PAzo-L/D-3 were obtained first in tetrahydrofuran (THF, good solvent).

The CD spectrum of PAzo-L-3 showed a negative bisignate Cotton effect (the sign refers to the longer wavelength of the two extrema) and PAzo-D-3 had a mirror image of the positive bisignate Cotton effect (Fig. 1a). The bisignate Cotton effect is typical of exciton coupling due to cooperative dipole–dipole interactions between asymmetrical side-chain Azo units.[37,38] Meanwhile, the above chiroptical property in a dissolved state was further verified in different good solvents, including benzene, 1,2-dichloroethane (DCE), trichloromethane, dichloromethane and dimethyl sulfoxide, demonstrating that PAzo-L-3 possessed very similar exciton-coupled chiral characteristics (Fig. S4†). Unlike in a macromolecular-dissolved state, by adding methylcyclohexane (MCH, poor solvent) to the DCE solution of PAzo-L-3, the polymer aggregates were gradually formed due to the minimization of the energetically unfavourable hydrophobe-solvent interactions. The intensity of the bisignate CD spectra continuously changed with the increasing MCH content, as shown in Fig. 1b. Interestingly, the CD signal centered at 367 nm gradually changed from a negative to a positive effect. This indicated that an unexpected chiroptical inversion happened when PAzo-L-3 changed from the dissolved state to the aggregated state. The authenticity of circular dichroism was confirmed by the negligible LD artifacts in the aggregated state (Fig. S5†). *Vice versa*, PAzo-D-3 showed a similar chiroptical inversion but with the reverse helical direction (Fig. S6a†).

Supplementary experiments were further performed to identify the chirality of PAzo-L-3 in both macromolecular-dissolved and aggregated states, respectively. First, the effect of PAzo-L-3 concentration (0.005–0.03 mg mL^{-1}) in THF (good solvent) on CD intensity was investigated (Fig. S7†). It is well known that supramolecular-aggregated chirality is highly sensitive to the concentration of polymers, but the opposite is true for macromolecular-dissolved chirality. The linear dependence of CD intensity on the polymer concentration indicated that the

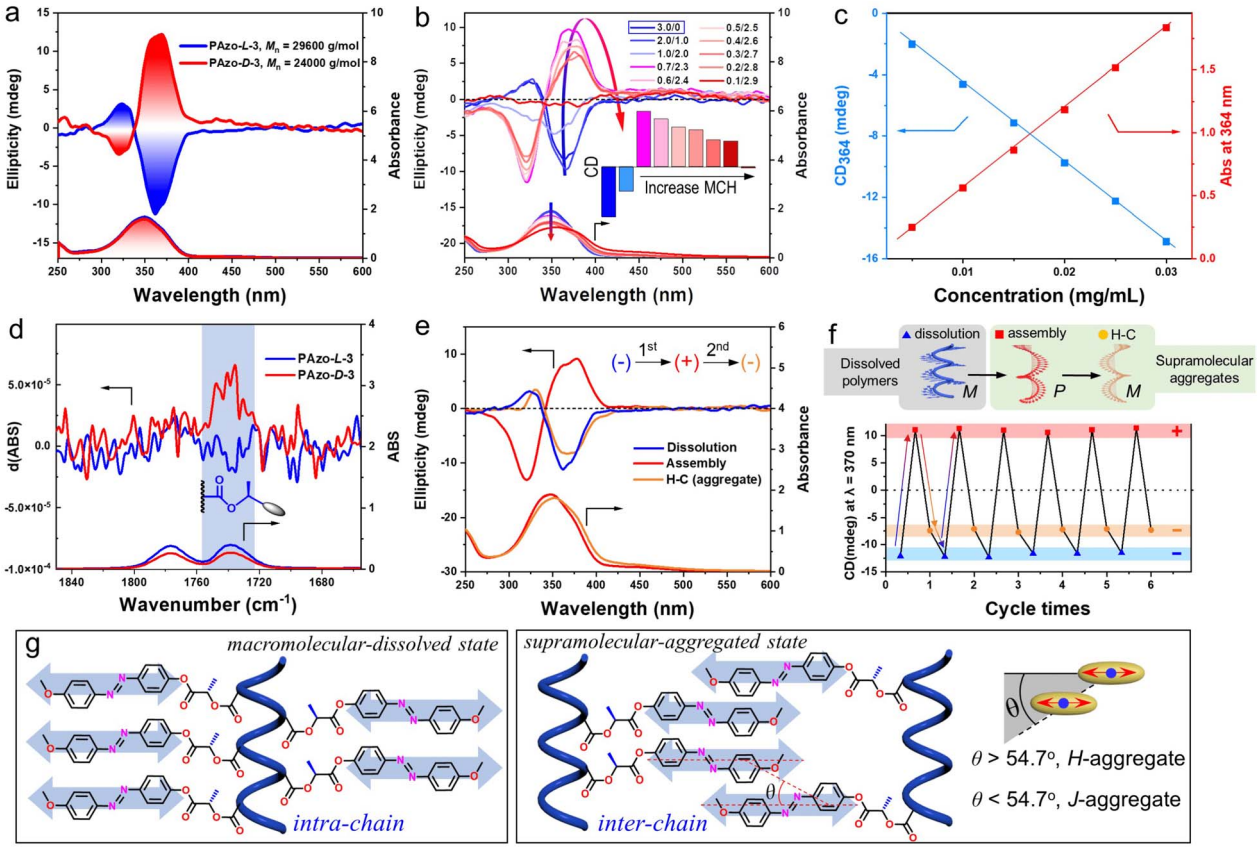

Fig. 1 (a) CD and UV-vis spectra of PAzo-L/D-3 in THF. (b) CD and UV-vis spectra of PAzo-L-3 in DCE/MCH mixed solvents with different volume ratios. (c) Plots of CD and UV-vis absorption intensity values at 364 nm with the concentration of PAzo-L-3 in THF at 20 °C. (d) The IR and VCD spectra of PAzo-L/D-3 in THF-d_8. (e) CD and UV-vis spectra of PAzo-L-3 in dissolution (DCE), in assembly (DCE/MCH = 0.6/2.4, v/v) and after heating–cooling (H–C) treatment. (f) The chiroptical switch with triple transitions. The steps of the operation are first dissolution (–) and then assembly at room temperature (+), followed by heating–cooling (–) of PAzo-L-3. (g) The molecular packing and macromolecular geometry in dissolved and aggregated states, respectively.

optical activity of the dissolved Azo units came from the external Azo units along the helical backbone (macromolecular chirality) rather than from supramolecular-aggregated chirality (supramolecular chirality) (Fig. 1c).[39] Second, the specific optical rotation ($[\alpha]_D^{25}$) of PAzo-L-3 was about eleven times higher than that of its monomer (Table S1†), demonstrating that the specific optical rotation of the polymer was not only from the configurational chirality, but also from a higher-order helical structure, most likely the secondary structure of the main-chain helix.[40] The enhancement of optical rotation of the polymer can be ascribed to the helical structure of the polymer backbone. Third, infrared spectroscopy (IR) and vibratory circular dichroism (VCD) were also employed to reveal the chiroptical differences. As shown in Fig. 1d and S8,† the obvious VCD signal in the carbonyl group near the main-chain could also be attributed to the formation of a helical polymer backbone compared to their monomers.

Furthermore, when the chiral stereocenter is not located between the main-chain and Azo unit but attached to the end of the Azo unit, the macromolecular-dissolved polymer was CD-silent as previous studies presented.[41,42] Oriol *et al.* reported that the backbone helicity was difficult to induce when the side-chain chiral stereocenter was far away from the polymer backbone.[41] Based on the above analysis, in our study, the chiral stereocenter is close to the polymer backbone, so chiral properties in the macromolecular-dissolved state (DCE, single good solvent) are due to a helical conformation of the polymer backbones (secondary chirality), which drives the side-chain Azo units to be arranged in the helix within the chain (Scheme 1, intra Int_M of the backbone and intra Ext_M of Azo). Accordingly, the negative-to-positive inversion of CD signals in Fig. 1b can be regarded as the chirality inversion from the intra-chain helix of Azo along the backbones to the inter-chain helix of Azo in a supramolecular-aggregated state (Scheme 1, intra Int_M of the backbone, intra Ext_M of Azo and inter Ext_P of Azo). The Cotton effect is located in the absorption region of Azo units. When two (or more) Azo chromophores are aggregated in local space and have an appropriate asymmetric stacking, these two units electrically allow π–π* transitions to interact with each other to generate CD effects.

More interestingly, a second chiroptical inversion of PAzo-L/D-3 aggregates was found after thermal treatment. As presented in Fig. 1e and S6b,† the positive (negative) CD signal (centered at 375 nm, the first Cotton band) of PAzo-L(D)-3 aggregates in DCE/MCH (0.6/2.4, v/v) solvents was inversed to a negative

(positive) one, when the aggregates were heated at 80 °C for 10 min and then cooled down to room temperature (heating–cooling, H–C). Since the polymer PAzo-L-3 underwent two chiral inversions throughout three states, a chiroptical switch including triple transitions can be constructed in this system by changing the external conditions (from dissolution-to-assembly-to-H–C). After screening various conditions (Fig. 1f and S9†), the CD signal of PAzo-L-3 was negative in DCE, which then transited to positive when poor MCH solvent was added to the DCE solution. Subsequently, the CD signal was changed from positive to negative again after H–C of the aggregated assembly, which then returned to the initial state without fatigue after redissolving the polymer aggregates. Through the above repeating operations, we successfully performed chiroptical transitions at least six times.

The changes in CD signals indicated that the mechanisms for the multiple chiroptical inversions are essentially different (Fig. 1g). We further analysed the molecular packing and macromolecular geometry during chiroptical inversions using UV-vis absorption spectra. For Azo-polymers, the formation of *H*- and *J*-aggregates is known to cause blue-shift and red-shift of the UV-vis absorption in the range of the π–π* transition band, respectively.[42–45] When the first chiroptical inversion of PAzo-L-3 occurred from macromolecular-dissolved chirality to supramolecular-aggregated chirality, a broadened blue-shifted UV-vis absorption band was observed, demonstrating the dominant formation of *H*-aggregates (Fig. S10a†). Meanwhile, in the process of second chiroptical inversion caused by H–C, the UV-vis absorption of the supramolecular aggregates was obviously red-shifted relative to that before the thermal treatment (Fig. S10b†). The red-shifted absorption indicated the conversion of *H*-aggregates to *J*-aggregates. Therefore, the first chiroptical inversion could be ascribed to the transition from intra-chain macromolecular chirality in a completely dissolved state (helical conformation of coupled Azo units) to supramolecular chirality in inter-chain interacted *H*-aggregation (θ > magic angle 54.7°, Fig. 1g), while the second chiroptical inversion is due to the formation of dominant supramolecular *J*-aggregates (θ < 54.7°). It also should be noted that the chiral stereocenter did not change during the experiment, so the PAzo-L-3 aggregates contain both internal intra-chain helicity and external inter-chain helicity, while the PAzo-L-3 supramolecular-aggregated assemblies showed positive CD signals. It can be ascribed to the additivity principle of the pair-wise interactions that the CD spectrum of PAzo-L-3 aggregates is a summation of one significant contribution due to inter-chain supramolecular stacks with a positive exciton chirality and one close to smaller negative signals due to the intra-chain macromolecular stacks.

By adding poor solvent to the DCE solution, the macromolecular chirality is transformed into a supramolecular H-helix due to the aggregation of Azo units between polymer chains, exhibiting the first chiroptical inversion. This supramolecular H-helix is then transformed to the *J*-aggregate by thermal annealing, which exhibited the second inverted chiroptical signal. Furthermore, time-dependent experiments show that the CD signal of the supramolecular H-helix (the one that is formed after the first inversion) gradually decreased, indicating that it is maintained by the interaction between different polymer chains in the kinetic state. However, the supramolecular *J*-aggregate, the one that is formed after the second inversion, is in a thermodynamically stable state such that its chiral signal remained unattenuated for a long time (Fig. S11†). Because PAzo-L-3 experienced three states of chiral expression, the CD signs before the first inversion and after the second inversion are all negative (Fig. S12a†). To distinguish the origin of bisignate CD signals in these two negative states, we further performed filtration experiments.[32] As shown in Fig. S12b,† the CD signal and UV-vis absorption of PAzo-L-3 in DCE solution before and after filtration were basically unchanged. However, the CD signal of *J*-aggregates completely disappeared after the filtering operation (Fig. S12c†). Such experimental results are also consistent with the above transition mechanisms. In other words, the initial chiral properties originated from intra-chain Azo coupling along with the helical backbone in dissolved DCE solution, while the chiral properties of *H*- and *J*-aggregates are due to aggregation-induced circular dichroism between different polymer chains.

In addition, we also synthesized a comparative monomer MAzo-L-2 with a similar structure to MAzo-L-3 (monomer of PAzo-L-3) and prepared the corresponding polymer PAzo-L-2 by RAFT polymerization (Fig. 2a and S13†). Compared with PAzo-L-3, the distance from the stereocenter to the Azo unit was reduced by one C–C bond while that was increased by the same length to the polymer backbone, accordingly. We treated PAzo-L-2 in the same way as that of PAzo-L-3. As shown in Fig. 2b, the CD spectra of PAzo-L-2 showed a negative bisignate Cotton effect both in the fully dissolved state (pure DCE solvent) and in aggregated state (mixed DCE/MCH solvent). The macromolecular helicity in the

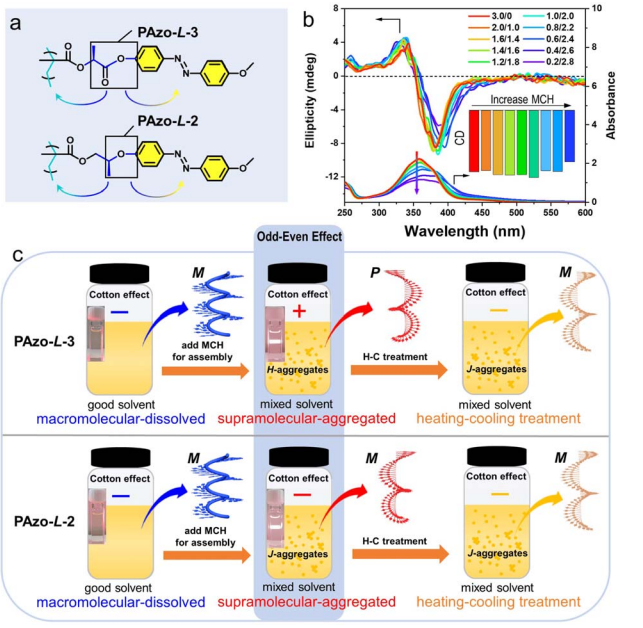

Fig. 2 (a) Chemical structures of PAzo-L-3 and PAzo-L-2. (b) CD and UV-vis spectra of PAzo-L-2 in mixed solvents with different volume ratios of DCE/MCH. (c) Schematic presentation of the corresponding Cotton effects and odd–even effects for polymers PAzo-L-3 and PAzo-L-2 in different states.

fully dissolved state still remained, and no chiroptical inversion was observed when the polymer PAzo-L-2 changed from a completely dissolved state to an aggregated state. These results indicated that the intra-chain helicity of Azo units in these two systems was not influenced by the distance between the chiral stereocenter and backbone, while the inter-chain helicity of Azo units is sensitive to the distance between the chiral stereocenter and the Azo unit. As a result, adjusting the distance from the chiral stereocenter to Azo chromophores can change the helical direction of supramolecular chiral assemblies, which was very similar to the chiral odd–even effect previously reported in small molecule and oligomer systems.[23,24,46,47] As presented in Fig. S13b,† the UV-vis absorption of PAzo-L-2 in an aggregated state (DCE/MCH = 0.6/2.4, v/v) had an obvious red-shift as compared to that in a completely dissolved state, indicating that it dominantly formed *J*-aggregates. Furthermore, no chiroptical inversion of PAzo-L-2 aggregates occurred even under the similar H–C treatment (Fig. S13c†). The different types of supramolecular-aggregated chirality in these two systems in mixed solvents can be regulated by the distance from the chiral stereocenter to the Azo unit (odd for PAzo-L-3 and even for PAzo-L-2), which also exhibited tunable chiral aggregation (*H*-aggregates for PAzo-L-3 and *J*-aggregates for PAzo-L-2, Fig. 2c). Therefore, we can control the chirality inversion of the Azo-polymers in the transition process from macromolecular helical chirality to supramolecular chirality and further regulate the chiroptical inversion in the supramolecular-aggregated state by adjusting the distance from the chiral stereocenter to the Azo unit.

It is well known that the Azo unit is a typical photo-responsive chromophore. The stable coplanar structure of *trans*-Azo can be converted to a bent *cis*-isomer under UV light irradiation, while *cis*-to-*trans* isomerization could be realized by visible light irradiation or heating treatment.[48–51] This unique dynamic property can be employed to construct the reversible chiroptical switch with "on–off" properties, in which the coplanar *trans*-Azo units form the helical stacks by π–π interactions while the bent *cis*-isomers may destroy the ordered helical stacks. In this study, the unique *trans–cis* isomerization of Azo units is employed to investigate the mechanisms of chirality transition and inversion. As shown in Fig. 3a and e, PAzo-L-3 dissolved in THF solution was irradiated with 365 nm UV light. The *trans*-Azo units gradually changed to *cis*-isomers with the increase in irradiation time, which caused the CD signal to fade out in 160 s. The following irradiation of 435 nm visible light converted the *cis*-Azo back to the *trans*-isomer and recovered the CD signal more than five times (Fig. 3b and S14†). Here, the partially interacting Azo units form helical structures that contribute to the CD signals. Therefore, the CD intensity shows no attenuation when part of the Azo units reconstructs the helical structures.

More interestingly, the CD signal showed a different changing tendency, when supramolecular-aggregated PAzo-L-3 in DCE/MCH mixed solvent (0.6/2.4, v/v) was irradiated with 365 nm UV light. During the process of UV light irradiation, the CD signals gradually decreased to nearly zero, and then inverted to negative maximum values at 100 s. Subsequently, the negative CD values decreased to zero again at 320 s (Fig. 3c). The

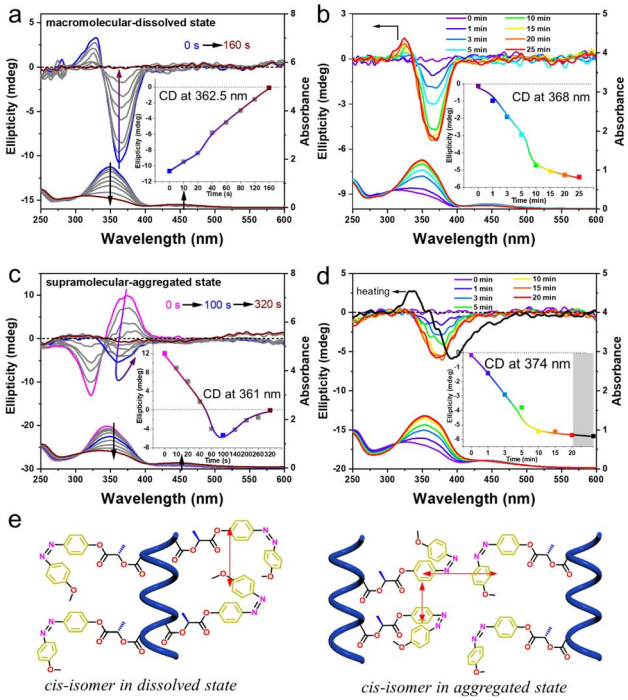

Fig. 3 (a) CD and UV-vis spectra of PAzo-L-3 irradiated with 365 nm UV light in THF. (b) CD and UV-vis spectra of PAzo-L-3 irradiated with 435 nm visible light in THF. (c) CD and UV-vis spectra of PAzo-L-3 irradiated with 365 nm UV light in DCE/MCH mixed solvent (0.6/2.4, v/v). (d) CD and UV-vis spectra of PAzo-L-3 irradiated with 435 nm visible light irradiation in DCE/MCH mixed solvent (0.6/2.4, v/v). (e) Schematic presentation of the *cis*-isomers and the destruction of intra-chain and inter-chain interactions.

results indicated that the intra-chain helical Azo structure along the polymer backbone remains unaltered, when the inter-chain supramolecular interaction is disrupted. Therefore, the supramolecular aggregates of PAzo-L-3 contain both intra-chain and inter-chain external Azo helicity, while the CD spectra exhibit positive signals due to the additivity principle of the pair-wise interactions. Since the content of bent *cis*-Azo gradually increased with UV light irradiation, the inter-chain supramolecular interaction was destroyed first before the intra-chain dipole–dipole interaction. Therefore, the CD signals of PAzo-L-3 supramolecular-aggregated assemblies underwent a reversal in the process of UV light irradiation (graph in the inset of Fig. 3c). Furthermore, only a negative Cotton effect, instead of the original positive one, was gradually recovered after the irradiation of 435 nm visible light (Fig. 3d), indicating that only the intra-chain macromolecular chirality could be recovered (Fig. 3e). Upon heating-assisted *cis–trans* isomerization (black line in Fig. 3d), the CD spectrum is basically similar in sign and amplitude except for the appearance of the wavelength splitting $\Delta\lambda_{max}$ (the distance between the peak and valley of the bisignate Cotton band according to Davydov splitting).[38]

The chiroptical properties of PAzo-L-2 and PAzo-L-3 indicated that the distance between the chiral stereocenter and the Azo unit in the side-chain can regulate the helical direction of the supramolecular stacks in an aggregated state. This interesting

phenomenon inspired us to explore the odd–even effect in modulating the chiroptical characteristics of the current polymer system. In the past few years, the studies on the odd–even effect have mainly focused on small molecular and oligomeric supramolecular systems or main-chain helical polymer systems.[23,24,46,47,52] There are few reports on the odd–even effect in supramolecular assembly of side-chain helical polymer systems due to the complexity of non-covalent interactions and macromolecular geometry. Therefore, a series of polymers PAzo-L/D-*m* (Scheme 1, $m = 6, 7, 8, 9, 10$, longer distance from the Azo unit to the chiral stereocenter) were synthesized *via* RAFT polymerization.

The CD results above indicated that PAzo-L/D-3 had obvious chiroptical expression in good solvent; however, all the other series of polymers PAzo-L/D-*m* ($m = 6, 7, 8, 9, 10$) were CD-silent in the dissolved state (Fig. S15†). Similar to PAzo-L/D-3, the VCD spectra and optical rotation of the PAzo-L/D-10 main-chain in the dissolved state still maintained an internal helical conformation (Fig. S8 and Table S1†). The helical conformation of the polymer main-chain is still driven by the chiral stereocenter, and thus unchanged due to the constant distance from the chiral stereocenter to the main-chain backbone. However, the alkyl spacers introduced between the stereocenter and the Azo units increase the freedom of the side-chain Azo units, and consequently, the polymer PAzo-L/D-*m* ($m = 6, 7, 8, 9, 10$) series were CD-silent in the dissolved state.

Although the Azo groups in the PAzo-L/D-*m* ($m = 6, 7, 8, 9, 10$) series are not well oriented in the dissolved state, once the aggregate is formed, a chiral arrangement is produced and commanded by the chiral stereocenter of the polymer. After adding MCH to the DCE solution of the polymer, the morphologies of polymer aggregates were first characterized by transmission electron microscopy (TEM) (Fig. S16†). For all polymers including PAzo-L-3, the morphologies of the polymer assemblies changed from spherical aggregates to irregular aggregates with an increase in the MCH content in the mixed solvent. Furthermore, it is interesting to find that the supramolecular assemblies formed by PAzo-L-*m* ($m = 6, 8$, and 10, even number) exhibited negative bisignate Cotton effects, while those formed by polymers PAzo-L-*m* ($m = 3, 7$, and 9, odd number) showed positive bisignate Cotton effects (Fig. 4a–e). The corresponding Azo-polymers of the D-configuration exhibited mirror-image CD spectra to their counterparts of the L-configuration (Fig. S17†). The results indicated that the chirality transfer in the supramolecular-aggregated state occurred successfully and external Azo helicity in different polymer chains was inverted with the length of the spacer (*i.e.*, from inter Ext_P to inter Ext_M of Azo in Scheme 1).

The chirality transition in these polymer assemblies can be summarized by SED/SOL-rules that were originally developed for cholesteric liquid crystals (*S* is the absolute spatial configuration of the chiral stereocenter, E or O is the atom count from the chiral stereocenter to the core, and D or L is the handedness of the helical structure).[46,47] For example, the polymer PAzo-L-10 was in the *S* configuration (L-methyl lactate) with ten atoms (even number) from the chiral stereocenter to the Azo unit. According to the SED/SOL-rules, the supramolecular stacks

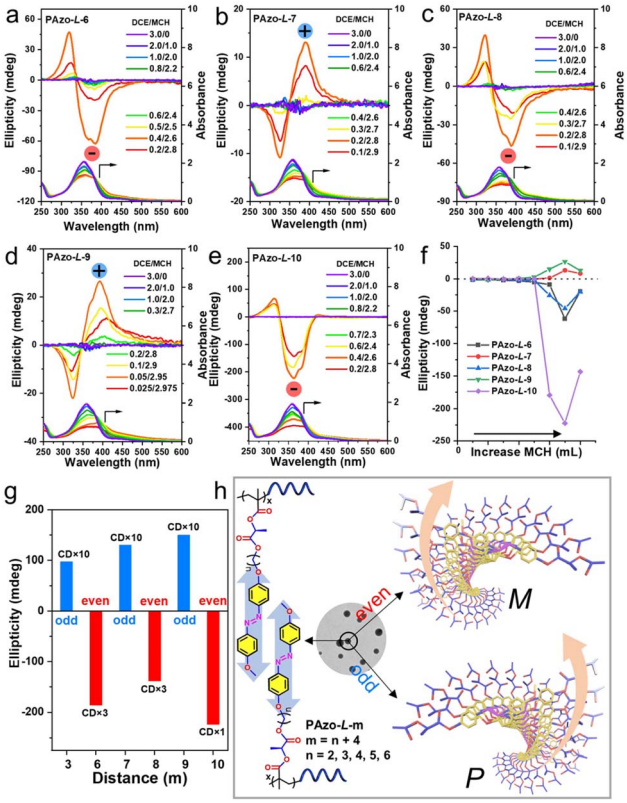

Fig. 4 (a–e) CD and UV-vis spectra of PAzo-L-*m* ($m = 6, 7, 8, 9, 10$) in mixed solvents with different volume ratios of DCE/MCH. (f) Maximum values of the first Cotton effects of PAzo-L-*m* supramolecular assemblies in an aggregated state. (g) Odd–even effect of PAzo-L-*m* supramolecular assemblies. "CD × 10" represents the maximum value of the first Cotton effect multiplied by 10. (h) Schematic presentation of the inter-chain supramolecular helical stacks of PAzo-L-*m* in an aggregated state.

should be a left-handed helix (dextro) and exhibit a negative Cotton effect (Fig. 4e). Meanwhile, the chiroptical expression of the supramolecular assemblies strongly depends on the content of MCH solvent; the maximum CD values of each polymer aggregate both increased gradually with the relative DCE/MCH volume value and then decreased after reaching their maximum values (Fig. 4f and S18†). Furthermore, the CD maximum values exhibit alternating inversion signs with the odd–even alternation of the distances from the chiral stereocenter to the Azo unit (Fig. 4g). The current work extended the odd–even effect into side-chain polymer systems, and the handedness of the Azo supramolecular stacks can be modulated by the internal structural changes of Azo-polymers (Fig. 4h). For Azo-polymers with odd lengths, the supramolecular assemblies possess a right-handed (P-type) helix. In contrast, Azo-polymers with even lengths exhibit a left-handed (M-type) helix. From the results above, it was found that the chirality transition and inversion in Azo-polymers can be regulated not only by dissolution–aggregation in molecular-level differentiations but also by photo-triggered *trans–cis* isomerization of the Azo units and by the odd–even effect in internal structural changes.

Conclusions

In conclusion, we achieved chirality control and expanded the applicability of the odd–even effect into side chain Azo-polymer systems for the first time. The mechanisms of the chiroptical transitions and inversions in Azo-polymers were elucidated through systematic analysis of the molecular packing and macromolecular geometry. In other words, modulating the intra-chain macromolecular helix along the backbone and inter-chain supramolecular helix of Azo units is the key to control the hierarchical chiroptical expression. Furthermore, two different chiroptical switches, one with multiple inversion properties regulated by dissolution–aggregation differentiations and the other with "on–off" properties triggered by *trans–cis* Azo isomerization, have been successfully constructed in one system. In addition, controllable chiroptical inversion of supramolecular stacks was realized in the side-chain polymer systems by tuning the odd–even spacer lengths between the chiral stereocenter and the Azo unit. This work reveals the chirality transition and inversion at the molecular, macromolecular and supramolecular levels, which will open up new ideas for the design of advanced chirality-controllable materials.

Data availability

The experimental data can be found in the ESI† and manuscript and is referred to throughout the manuscript.

Author contributions

Y. F. Ma, X. X. Cheng and Prof. W. Zhang conceived the research idea and co-wrote the original draft. Y. F. Ma, X. X. Cheng, Z. X. He and H. T. Ma performed the synthesis and characterization. Prof. W. Zhang and Prof. Z. B. Zhang co-revised the manuscript.

Conflicts of interest

There are no conflicts to declare.

Acknowledgements

The authors are grateful for the financial support from the National Nature Science Foundation of China (92056111, 21971180 and 21925107), Nature Science Key Basic Research of Jiangsu Province for Higher Education (No. 19KJA360006), the Priority Academic Program Development (PAPD) of Jiangsu Higher Education Institutions and the Program of Innovative Research Team of Soochow University.

Notes and references

1 L. D. Barron, *Space Sci. Rev.*, 2008, **135**, 187.
2 M. H. Liu, L. Zhang and T. Y. Wang, *Chem. Rev.*, 2015, **115**, 7304.
3 C. Xu, Q. J. Lin, C. Shan, X. Han, H. Wang, H. Wang, W. J. Zhang, Z. Chen, C. X. Guo, Y. H. Xie, X. J. Yu, B. Song, H. Song, L. Wojtas and X. P. Li, *Angew. Chem., Int. Ed.*, 2022, **61**, e202203099.
4 Y. Sang and M. Liu, *Chem. Sci.*, 2022, **13**, 633.
5 J. Wang, C. Y. Li, S. Jin, X. Weng, R. M. Van Horn, M. J. Graham, W.-B. Zhang, K.-U. Jeong, F. W. Harris, B. Lotz and S. Z. D. Cheng, *Ind. Eng. Chem. Res.*, 2010, **49**, 11936.
6 R. M. Ho, M. C. Li, S. C. Lin, H. F. Wang, Y. D. Lee, H. Hasegawa and E. L. Thomas, *J. Am. Chem. Soc.*, 2012, **134**, 10974.
7 C. Y. Li, S. Z. D. Cheng, X. Weng, J. J. Ge, F. Bai, J. Z. Zhang, B. H. Calhoun, F. W. Harris, L.-C. Chien and B. Lotz, *J. Am. Chem. Soc.*, 2001, **123**, 2462.
8 L. Zhang, H.-X. Wang, S. Li and M. Liu, *Chem. Soc. Rev.*, 2020, **49**, 9095.
9 G. F. Liu, X. Li, J. H. Sheng, P.-Z. Li, W. K. Ong, S. Z. F. Phua, H. Agren, L. L. Zhu and Y. L. Zhao, *ACS Nano*, 2017, **11**, 11880.
10 H. K. Bisoyi and Q. Li, *Angew. Chem., Int. Ed.*, 2016, **55**, 2994.
11 J. Kim, J. Lee, W. Y. Kim, H. Kim, S. Lee, H. C. Lee, Y. S. Lee, M. Seo and S. Y. Kim, *Nat. Commun.*, 2015, **6**, 6959.
12 H. J. Jiang, Y. Q. Jiang, J. L. Han, L. Zhang and M. H. Liu, *Angew. Chem., Int. Ed.*, 2019, **58**, 785.
13 A. Gopal, M. Hifsudheen, S. Furumi, M. Takeuchi and A. Ajayaghosh, *Angew. Chem., Int. Ed.*, 2012, **51**, 10505.
14 K. Maeda, H. Mochizuki, M. Watanabe and E. Yashima, *J. Am. Chem. Soc.*, 2006, **128**, 7639.
15 R. S. Johnson, T. Yamazaki, A. Kovalenko and H. Fenniri, *J. Am. Chem. Soc.*, 2007, **129**, 5735.
16 Y. W. Huang, J. C. Hu, W. F. Kuang, Z. X. Wei and C. F. J. Faul, *Chem. Commun.*, 2011, **47**, 5554.
17 N. Ousaka, Y. Takeyama and E. Yashima, *Chem. Sci.*, 2012, **3**, 466.
18 Q. Ye, F. Zheng, E. Zhang, H. K. Bisoyi, S. Zheng, D. Zhu, Q. Lu, H. Zhang and Q. Li, *Chem. Sci.*, 2020, **11**, 9989.
19 S. Zahn and J. W. Canary, *Science*, 2000, **288**, 1404.
20 E. Suárez-Picado, E. Quiñoá, R. Riguera and F. Freire, *Angew. Chem., Int. Ed.*, 2020, **59**, 4537.
21 N. Marino, D. Armentano, E. Pardo, J. Vallejo, F. Neve, L. Di Donna and G. De Munno, *Chem. Sci.*, 2015, **6**, 4300.
22 S. Kobayashi, K. Morino and E. Yashima, *Chem. Commun.*, 2007, 2351.
23 J. Y. Liu, F. Yuan, X. Y. Ma, D.-i. Y. Auphedeous, C. L. Zhao, C. T. Liu, C. Y. Shen and C. L. Feng, *Angew. Chem., Int. Ed.*, 2018, **57**, 6475.
24 R. Marty, R. Nigon, D. Leite and H. Frauenrath, *J. Am. Chem. Soc.*, 2014, **136**, 3919.
25 J. G. Zhi, Z. G. Zhu, A. H. Liu, J. X. Cui, X. H. Wan and Q. F. Zhou, *Macromolecules*, 2008, **41**, 1594.
26 E. R. Lermo, B. M. W. Langeveld-Voss, R. A. J. Janssen and E. W. Meijer, *Chem. Commun.*, 1999, 791.
27 R. Rodríguez, E. Suárez-Picado, E. Quiñoá, R. Riguera and F. Freire, *Angew. Chem., Int. Ed.*, 2020, **59**, 8616.
28 R. Rodríguez, E. Quiñoá, R. Riguera and F. Freire, *Chem. Mater.*, 2018, **30**, 2493.
29 E. Yashima, K. Maeda, H. Iida, Y. Furusho and K. Nagai, *Chem. Rev.*, 2009, **109**, 6102.

30 F. Freire, J. M. Seco, E. Quiñoá and R. Riguera, *Angew. Chem., Int. Ed.*, 2011, **50**, 11692.
31 T. Nakano and Y. Okamoto, *Chem. Rev.*, 2001, **101**, 4013.
32 Z. Fernández, B. Fernández, E. Quiñoá and F. Freire, *J. Am. Chem. Soc.*, 2021, **143**, 20962.
33 Z. Fernández, B. Fernández, E. Quiñoá, R. Riguera and F. Freire, *Chem. Sci.*, 2020, **11**, 7182.
34 N. Suzuki, M. Fujiki, R. Kimpinde-Kalunga and J. R. Koe, *J. Am. Chem. Soc.*, 2013, **135**, 13073.
35 Y. Nakano, F. Ichiyanagi, M. Naito, Y. Yang and M. Fujiki, *Chem. Commun.*, 2012, **48**, 6636.
36 V. N. Malashkevich, R. A. Kammerer, V. P. Efimov, T. Schulthess and J. Engel, *Science*, 1996, **274**, 761.
37 A. Painelli, F. Terenziani, L. Angiolini, T. Benelli and L. Giorgini, *Chem.–Eur. J.*, 2005, **11**, 6053.
38 G. Albano, G. Pescitelli and L. Di Bari, *Chem. Rev.*, 2020, **120**, 10145.
39 J. H. Chu, X. H. Xu, S. M. Kang, N. Liu and Z. Q. Wu, *J. Am. Chem. Soc.*, 2018, **140**, 17773.
40 J. X. Cui, X. C. Lu, A. H. Liu, X. H. Wan and Q. F. Zhou, *Macromolecules*, 2009, **42**, 7678.
41 J. del Barrio, R. M. Tejedor, L. S. Chinelatto, C. Sánchez, M. Piñol and L. Oriol, *J. Mater. Chem.*, 2009, **19**, 4922.
42 X. X. Cheng, T. F. Miao, Y. F. Ma, X. Y. Zhu, W. Zhang and X. L. Zhu, *Angew. Chem., Int. Ed.*, 2021, **60**, 24430.
43 G. F. Liu, J. H. Sheng, H. W. Wu, C. L. Yang, G. B. Yang, Y. X. Li, R. Ganguly, L. L. Zhu and Y. L. Zhao, *J. Am. Chem. Soc.*, 2018, **140**, 6467.
44 S. Wu, L. F. Niu, J. Shen, Q. J. Zhang and C. Bubeck, *Macromolecules*, 2009, **42**, 362.
45 X. Tong, L. Cui and Y. Zhao, *Macromolecules*, 2004, **37**, 3101.
46 G. W. Gray and D. G. McDonnell, *Mol. Cryst. Liq. Cryst.*, 1977, **34**, 211.
47 J. W. Goodby, *J. Mater. Chem.*, 1991, **1**, 307.
48 H.-L. Sun, Y. Chen, J. Zhao and Y. Liu, *Angew. Chem., Int. Ed.*, 2015, **54**, 9376.
49 X. X. Cheng, T. F. Miao, L. Yin, Y. J. Ji, Y. Y. Li, Z. B. Zhang, W. Zhang and X. L. Zhu, *Angew. Chem., Int. Ed.*, 2020, **59**, 9669.
50 G. Zhang, X. X. Cheng, Y. F. Wang and W. Zhang, *Aggregate*, 2022, e262, DOI: **10.1002/agt2.262**.
51 Y. J. Gan, H. B. Dai, Y. F. Ma, X. X. Cheng, Z. Wang and W. Zhang, *Macromolecules*, 2022, **55**, 8556.
52 J. W. Goodby, *Science*, 1986, **231**, 350.